Dynamical Signatures of Quasiparticle Interactions in Quantum Spin Chains

Anna Keselman,[1] Leon Balents,[1,2] and Oleg A. Starykh[3]
[1]*Kavli Institute for Theoretical Physics, University of California, Santa Barbara, California 93106, USA*
[2]*Canadian Institute for Advanced Research, Toronto, Ontario M5G 1M1, Canada*
[3]*Department of Physics and Astronomy, University of Utah, Salt Lake City, Utah 84112, USA*

(Received 29 May 2020; accepted 23 September 2020; published 27 October 2020)

We study the transverse dynamical susceptibility of an antiferromagnetic spin-$1/2$ chain in the presence of a longitudinal Zeeman field. In the low magnetization regime in the gapless phase, we show that the marginally irrelevant backscattering interaction between the spinons creates a nonzero gap between two branches of excitations at small momentum. We further demonstrate how this gap varies upon introducing a second neighbor antiferromagnetic interaction, vanishing in the limit of a noninteracting "spinon gas." In the high magnetization regime, as the Zeeman field approaches the saturation value, we uncover the appearance of two-magnon bound states in the transverse susceptibility. This bound state feature generalizes the one arising from string states in the Bethe ansatz solution of the integrable case. Our results are based on numerically accurate, unbiased matrix-product-state techniques as well as analytic approximations.

DOI: 10.1103/PhysRevLett.125.187201

Introduction.—The nearest-neighbor antiferromagnetic spin-$1/2$ chain [1] serves as a paradigmatic model of strongly correlated systems. In particular, it is an established setting in which the existence of *fractionalized* quasiparticles, deemed spinons, is incontrovertible. Spinons are the elementary excitations for magnetic fields below the critical saturation field, above which the ground state becomes fully polarized. In the saturated regime, the elementary excitations are instead simple (not fractionalized) magnons, or spin waves. A quasiparticle is, by definition, an excitation which, when isolated, propagates freely with minimal decay. However, in general, when multiple quasiparticles are present, they interact, and in a strongly correlated system, they interact strongly. Such interactions are present both for fractionalized and ordinary excitations, but impact the physics particularly strongly in the former case, as any local operator creates in this case more than one quasiparticle.

In this manuscript, we focus on dynamical signatures, i.e., features in the frequency-dependent spin correlations, of such quasiparticle interactions, in the presence of a magnetic field. Extensive numerical studies [2–7] of the dynamical correlation functions have been carried out in the Heisenberg limit, for which a Bethe ansatz solution exists. Consequently, the general structure of the correlations, and their deconstruction in terms of spinons, is already well established. Here, we go beyond the integrable limit, and add to this broad picture a detailed analytical theory of the effects of quasiparticle interactions, in both the low and high magnetic field (magnetization) regimes. Specifically, in the low magnetization case, we employ a continuum field theory in which spinon interactions are parametrized by the marginally irrelevant current-current backscattering coupling g. We show that this coupling creates a gap between two branches of excitations at zero momentum, which is equal to gM, where M is the magnetization, thus directly revealing the strength of interactions between spinons. We note that the fermionic field theory used here and the results we obtain for it have a direct parallel to a recent study by two of us on two dimensional spin liquids with a spinon Fermi surface [8]. The results herein thus serve in part as a proof of principle for the two dimensional case, with the major advantage that here the results are vetted by unbiased numerical simulations.

In the regime of large magnetization, the natural quasiparticles are spin flip magnons (spins antialigned with the field), leading to a dominant single branch in the dynamical susceptibility. We show, however, that two-magnon bound states appear as an additional higher energy branch due to interaction of the "probe" magnon with those already present in the ground state. The spectral weight of this higher energy branch is thus directly proportional to the strength of interactions, as well as the density of ground state magnons. Previous studies of the Heisenberg chain [2,3] have indeed identified the Bethe ansatz string to be related to two-magnon bound states in the high magnetization regime. However, here we show that this is not unique to the integrable chain limit, and provide a simple understanding which does not require the specialized Bethe ansatz formalism.

We test these analytical predictions by comparison to computations using numerical matrix-product-state (MPS) techniques [9]. In the small magnetization regime,

pdfelement
The Trial Version

 © 2020 American Physical Society

we tune the spinon interaction g by including a second-neighbor exchange coupling J_2, while in the large magnetization regime, magnon-magnon interactions are tuned by introducing magnetic anisotropy of the XXZ form. In both limits matrix-product-state calculations compare excellently with the theoretical predictions as the respective parameters controlling the density of quasiparticles and the strength of interactions between them are varied.

Model.—We consider a spin-1/2 chain, with antiferromagnetic nearest-neighbor coupling, $J_1 > 0$, and next-nearest-neighbor coupling J_2 in longitudinal Zeeman field B. The Hamiltonian of the system is given by

$$H = \sum_i J_1(\vec{S}_i \cdot \vec{S}_{i+1})_\eta + J_2(\vec{S}_i \cdot \vec{S}_{i+2})_\eta - BS_i^z, \tag{1}$$

where $\vec{S}_i$ is a spin-1/2 operator on site i. We allow for anisotropic interactions and denote $(\vec{S}_i \cdot \vec{S}_j)_\eta \equiv S_i^x S_j^x + S_i^y S_j^y + \eta S_i^z S_j^z$. In the isotropic case, $\eta = 1$, and for $B = 0$, the system undergoes a phase transition at $J_2 = J_{2,c} \approx 0.241 J_1$, between a gapless and a dimerized phase [10,11]. In the following we will consider the regime $J_2 \leq J_{2,c}$ in which the system remains gapless.

We study the transverse susceptibility $\chi^\pm(k,\omega)$ imaginary part of which determines dynamical structure factor $S^{+-}(k,\omega)$ of the dynamical correlations at zero temperature, namely

$$\begin{aligned} S^{+-}(k,\omega) &= \int_{-\infty}^{\infty} dt e^{i\omega t} \sum_{j=-\infty}^{\infty} e^{-ikj} \langle S_j^+(t) S_0^-(0)\rangle \\ &= \sum_m |\langle m|S_k^-|0\rangle|^2 \delta(\omega - E_m), \end{aligned} \tag{2}$$

where $|0\rangle$ denotes the ground state of the system.

Our numerical calculations are carried out using the ITensor library [12]. To obtain the spectral function (2) we first obtain the ground state of the system using density matrix renormalization group (DMRG) [13]. We then perform time evolution up to times $t_{\max} = 80 J_1^{-1}$ using time-evolution block-decimation (TEBD) [14]. Our analysis is done on finite systems of length $N = 400$ sites with open boundary conditions [15,16].

Low magnetization.—In the discussion below we focus on the isotropic case, i.e., $\eta = 1$. The low energy effective description of the J_1–J_2 chain is given by an $\mathrm{SU}(2)_1$ Wess-Zumino-Witten conformal field theory. As discussed in Refs. [18–20], this theory has a convenient fermion representation which is faithful and simple for the Hamiltonian and spin currents we study here. We denote the right(left) moving fermionic spinons which constitute the low energy theory by $\psi_{R(L),s}$, where $s = \uparrow, \downarrow$ is the spin. The respective spin current is given by $\vec{J}_R = \frac{1}{2}\psi_R^\dagger \vec{\sigma} \psi_R$, where ψ_R denotes two-component spinor $\psi_R = (\psi_{R\uparrow}, \psi_{R\downarrow})^T$ (and similarly for ψ_L). The low energy Hamiltonian is given by $H = H_0 + V$, where H_0 corresponds to the noninteracting part

pdfelement
The Trial Version

$$H_0 = v \int dx [\psi_R^\dagger(-i\partial_x)\psi_R + \psi_L^\dagger(i\partial_x)\psi_L] \tag{3}$$

(here v is the Fermi velocity), and V is the backscattering interaction

$$V = -g \int dx [J_R^z J_L^z + \frac{1}{2} J_R^+ J_L^- + \frac{1}{2} J_R^- J_L^+]. \tag{4}$$

The Hamiltonian $H_0 + V$ appears as an interacting fermion problem for the spinons, an approach we will follow below. In a standard bosonization framework g gives rise to a nonlinear cosine term. In a renormalization group treatment, $g > 0$ is marginally irrelevant and as a function of its energy argument E flows logarithmically to zero at low energies [18,21,22], producing subtle logarithmic modifications to the temperature dependence of thermodynamic quantities such as susceptibility and specific heat [23–27]. The bare value of g depends on J_2 and changes sign at the critical value, i.e., $g \sim c(J_{2,c} - J_2)$ with $c > 0$ [11].

As we now show, the consequences of the nonzero $g > 0$ are more dramatic and directly evident in the spectral features in the presence of a Zeeman field. A longitudinal Zeeman field couples to the magnetization M, which is the sum of the right and left spin currents

$$H_B = -B \int dx M, \qquad M = J_R^z + J_L^z. \tag{5}$$

In the presence of the Zeeman field, renormalization group flow of g toward zero is cut off at $E = B$ [16,22,28] and moreover distinguishes the effects of the diagonal and spin flip components of the interactions in Eq. (4). Consequently, we must consider them separately and carefully. First, let us take $g = 0$ and introduce the Zeeman field B. In the spinon framework, the Zeeman field simply induces a spin splitting of the two spinon bands. The dynamical susceptibility is then

$$\chi_0^\pm(k,\omega) = \frac{M + \chi_0 vk}{\omega - B - vk} + \frac{M - \chi_0 vk}{\omega - B + vk} \xrightarrow[k\to 0]{} \frac{2M}{\omega - B}, \tag{6}$$

where $\chi_0 = 1/(2\pi v)$ is the noninteracting uniform susceptibility. There are two branches with linear dispersion and constant spectral weight, as shown by the dashed lines in Fig. 1. Note that the form at $k = 0$ is more robust than for $k > 0$, and is in fact exact provided the Hamiltonian in the absence of Zeeman field has SU(2) symmetry. This "Larmor theorem" [22] follows simply from the fact that in this case $[S_{\mathrm{tot}}^+, H] = BS_{\mathrm{tot}}^+$, where $S_{\mathrm{tot}}^+ = \sum_i S_i^+$.

Now consider the interaction g. Importantly, response at the energy of the order of the Zeeman energy B, see (6), is determined by $g = g(B) \neq 0$ in (4) which is small and

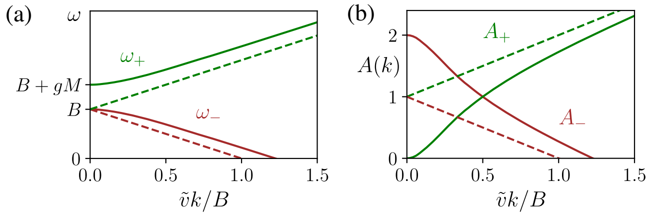

FIG. 1. Transverse susceptibility $\chi^{\pm}(k,\omega)$ obtained in the small k, and low magnetization regime. (a) The dispersion $\omega_{\pm}(k)$ is given by the green (brown) solid line for $gM/B = 1/2$ and green (brown) dashed line for $g = 0$. (b) The intensity of the upper (lower) branch $A_{\pm}$ is the green (brown) solid line for $gM/B = 1/2$ and green (brown) dashed line for $g = 0$.

finite. The diagonal $J^z_R J^z_L$ term in Eq. (4) leads for $M > 0$ to a simple increase of the spin splitting of the spinon bands by the energy $\Delta = gM/2$. Consequently, the full spin splitting is $B + \Delta$ and naively the poles in Eq. (6) would be shifted vertically to $B + \Delta \pm vk$. This clearly violates the Larmor theorem. The contradiction is resolved by including the spin flip part of the interaction $J^+_R J^-_L + \mathrm{H.c.}$, which results in the formation of a bound state between the particle and hole (exciton) created by the spin operator S^+. The two effects together are captured by a random phase approximation summation of ladder diagrams for the susceptibility, as described in [16], leading to the result

$$\chi^{\pm}(k,\omega) = M\left(\frac{A_+(k)}{\omega - \omega_+(k)} + \frac{A_-(k)}{\omega - \omega_-(k)}\right),$$
$$A_{\pm}(k) = 1 \pm \frac{\tilde{v}^2k^2 - B\Delta}{B\sqrt{\Delta^2 + \tilde{v}^2k^2}},$$
$$\omega_{\pm}(k) = B + \Delta \pm \sqrt{\Delta^2 + \tilde{v}^2k^2}. \tag{7}$$

Here $\tilde{v} = v\sqrt{1 - g^2\chi_0^2/4}$. This is plotted schematically in Fig. 1. The downward branch $\omega_-(k)$ has finite residue which approaches $2M$ for $k \to 0$ and $\omega_-(k) \to B$, satisfying the Larmor theorem. The spectral weight of the upward branch $\omega_+(k)$ vanishes quadratically $A_+(k) \propto \tilde{v}^2k^2$ for $k \to 0$, when $\omega_+(k) \to B + 2\Delta$. Both branches scale linearly with $\tilde{v}k$ for sufficiently large momenta $\tilde{v}k \gg \Delta$. Within our low energy approximation the $k = 0$ gap between the two branches is given by $2\Delta = \omega_+(0) - \omega_-(0) = gM$. Higher order in g and B contributions can modify it.

We now compare our analytical analysis to numerical results, which are consistent with earlier studies of the Heisenberg chain [3,5–7]. These works observed a finite gap, but did not address its origin and systematics. The dynamical correlations obtained numerically are shown in Fig. 2. As the spectral weight of the upper branch vanishes at $k = 0$, to obtain the gap 2Δ we extract the dispersion at small momenta [see Figs. 2(b) and 2(d)], fitting the two branches to the form expected from Eq. (7),

pdfelement
The Trial Version

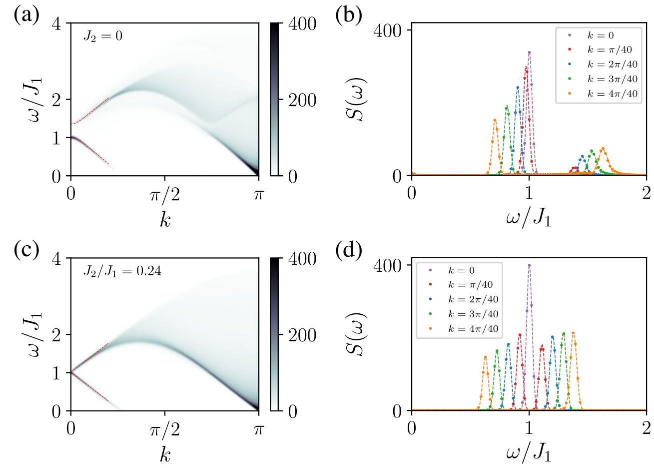

FIG. 2. Dynamical correlations $S^{+-}(k,\omega)$ obtained numerically for Zeeman field of $B/J_1 = 1$. (a),(b) $J_2 = 0$, (c),(d) $J_2/J_1 = 0.24$. In (a),(c) the red dashed line indicates a fit to the analytic expression in Eq. (7) valid in the vicinity of $k = 0$. In (b),(d) cuts of the dynamical correlations are shown for fixed values of k. Finite times used in the numerical time evolution lead to broadening of the spectral features beyond their intrinsic lineshape, as is apparent, e.g., for the response at $k = 0$.

and extrapolating to $k = 0$. The resulting gap versus magnetization, as J_2 is varied, is shown in Fig. 3(a). We account for higher order M^2 corrections to Δ by fitting the curves shown in Fig. 3 to the form $2\Delta = gM + \alpha M^2$, and extract $g(J_2)$ which is plotted in Fig. 3(b). Additional data for ferromagnetic $J_2 < 0$, which enhances g beyond that of the nearest-neighbor limit, is given in [16]. Extrapolating $g(J_2)$ to zero, we find that g vanishes at $J_2/J_1 = 0.239 \pm 0.005$ in agreement with the critical value $J_{2,c}/J_1 \approx 0.241$ [11] up to numerical uncertainties. Fixed momentum cuts of the $S^{+-}(k,\omega)$ [Figs. 2(b) and 2(d)] show that, as predicted by Eq. (7), the spectral weight of the upper branch is suppressed at small k for the Heisenberg case (the generic situation), while the two branches have approximately equal weight in the free spinon limit ($J_2 \approx J_{2,c}$).

High magnetization.—We next consider the limit of a nearly polarized chain with low density of down spins, i.e., when the field is close to saturation value $B_{\mathrm{sat}} = (1 + \eta)J_1$. In this limit it is useful to consider the mapping of spins to spinless fermions defined by $S^-_i = \prod_{j<i}(-1)^{n_j} c^{\dagger}_i$ and

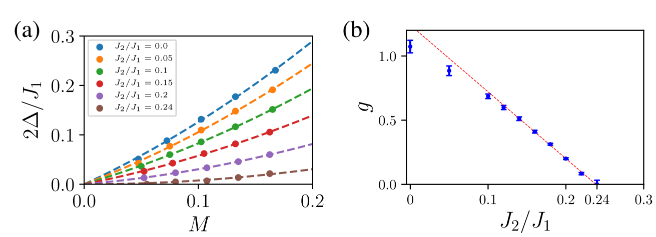

FIG. 3. (a) The splitting at $k = 0$ as function of the magnetization for different values of J_2. (b) The backscattering interaction g, extracted from 2Δ vs M in (a).

$S^z = 1/2 - n_i$, where $c_i^\dagger$ denotes the fermionic creation operator on site i and $n_i = c_i^\dagger c_i$. We focus on the case with $J_2 = 0$ first. The Hamiltonian (1) maps to

$$H = \sum_i \frac{J_1}{2}(c_i^\dagger c_{i+1} + \mathrm{H.c.}) + \eta J_1 n_i n_{i+1} + (B - \eta J_1) n_i. \quad (8)$$

At the saturation field $B = B_{\mathrm{sat}}$, the ground state is fully polarized, $|0\rangle = |FM\rangle$, and the only contribution to the dynamical susceptibility is the one-magnon state with momentum k, $|1_k\rangle = (1/\sqrt{N}) \sum_m e^{ikm} S_m^- |FM\rangle$. Consequently, the transverse correlations feature a sharp cosine mode at $\omega = J_1(1 + \cos k)$ as can be seen in Fig. 4(a). In the isotropic case, i.e., for $\eta = 1$, as the field is lowered and the density of spin down particles increases, we observe a splitting of the cosine mode as well as an appearance of a new mode at higher energies $\omega > 2J_1$ [see Fig. 4(b)]. To understand this response it is useful to compare to the limit of noninteracting fermions $\eta = 0$. The dynamical correlations obtained in this limit are plotted in Fig. 4(c). It is seen that the low energy response at $\omega < 2J_1$ is not altered significantly. Indeed, as shown in [16], the splitting of the lower mode can be understood in the noninteracting limit as originating from single particle excitations above the Fermi sea [29]. The mode at higher energies, however, is completely gone for $\eta = 0$, indicating that its presence comes purely from interaction effects. In fact, for the Heisenberg chain, it is known that this mode comes from Bethe ansatz string solutions, which can be identified as two-magnon bound states close to the saturation field [2,3]. Here, we show that it is a generic feature of the interacting magnons which exists beyond the integrable limit.

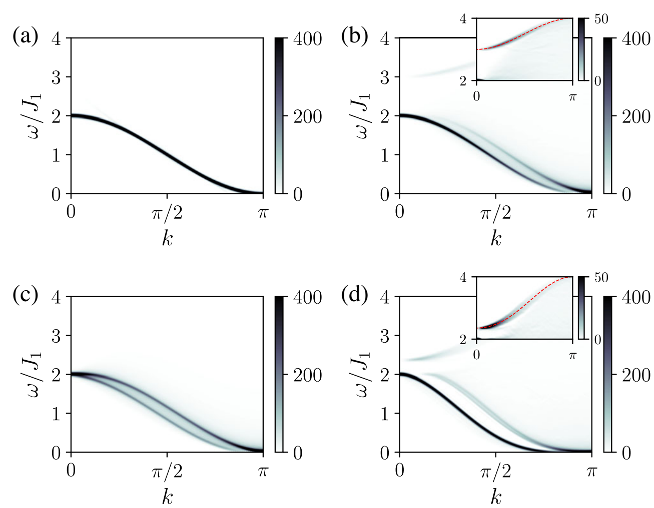

FIG. 4. Dynamical correlations $S^{+-}(k,\omega)$ obtained using density matrix renormalization group and time evolution in the high magnetization regime. In (a)–(c) we set $J_2 = 0$. (a) Saturated chain, i.e., $M = 1/2$, a pure cosine dispersion is observed. (b) $M = 0.45$ for an isotropic chain $\eta = 1$, (c) $M = 0.45$ in the noninteracting limit $\eta = 0$. (d) Isotropic chain $\eta = 1$ for $J_2/J_1 = 0.25$. In (b),(d) the inset shows the range $\omega > 2J_1$ of the response function on a different color scale that allows for better visibility of the high energy mode. The red dashed line corresponds to the two-magnon bound state dispersion $\epsilon_2(k + \pi)$.

pdfelement
The Trial Version

To examine two-particle bound state solutions we consider a state with two down spins

$$|2_K\rangle = \sum_{m,n} \psi_{m,n} S_m^- S_n^- |FM\rangle,$$
$$\psi_{m,n} \propto e^{iK[(m+n)/2]} f(m-n). \quad (9)$$

Because of translational invariance the two-particle wave function $\psi_{m,n}$ can be written as above, with K denoting the center of mass momentum of the pair of magnons. Looking for eigenstates of the Hamiltonian (1) of the form above, leads to an effective Schrodinger equation for $f(m-n)$. Requiring a bound solution (in which f decays at large argument) we can check that such a solution exists for a given K and obtain its energy, which lies above the two-particle continuum. For $J_2 = 0$ the dispersion of the bound state can be easily obtained analytically and is given by $\epsilon_2(K, J_2 = 0) = 2B - J_1 \sin^2(K/2)$ [1], while for finite J_2 we calculate the dispersion numerically [16].

To understand how the two-magnon bound states are revealed in the transverse correlations, we consider for simplicity the limit of a single down spin in the otherwise polarized ground state of length N. This state is a caricature of the many body ground state at a low density of spin flips $n_{\mathrm{SF}} = 1/2 - M = 1/N \ll 1$ close to but below the saturation field. Note that since the minimum of the single magnon dispersion is at momentum π for $J_1 > 0$ and $J_2/J_1 < 1/4$, the magnon present in the ground state will occupy that momentum. Hence, we take $|0\rangle = |1_\pi\rangle$ in Eq. (2). Now there is a contribution when $\langle m| = \langle 2_K|$ in Eq. (2), which, by momentum conservation, gives a matrix element $|\langle 2_K|S_k^-|1_\pi\rangle|^2 \propto \delta_{K,k+\pi}/N$ [16] (physically the $1/N$ factor appears because the spin flip created by S_k^- has only a small probability to occur near the spin flip already present in the ground state). This implies the appearance of response at energy $\omega = \epsilon_2(k + \pi)$ with an weight proportional to $1/N = 1/2 - M$ [16]. Plotting the expected dispersion due to the two-magnon bound state on top of the dynamical correlations obtained numerically [dashed line in Figs. 4(b) and 4(d)] we find an excellent agreement between the two [16]. We note that a similar argument has been used to explain the appearance of a bound state in the structure factor of a frustrated ladder upon slight magnetization of a gapped phase in Ref. [32].

Note that as opposed to the low magnetization regime, where the splitting between the modes at $k = 0$ vanishes at $J_2 \to J_{2,c}$, in the high magnetization regime the splitting between the modes remains finite, and from the aforementioned analysis is explicitly determined by the two-magnon bound state at $K = \pi$ [33,34] to be

$2\Delta = J_1 - 3J_2 + J_2^2/(J_1 - J_2)$ [16]. This highlights the fact that the nature and the origin of the high energy mode in the low and high magnetization regimes is very different. While in the low-magnetization regime the high energy mode describes a continuum of excitations and the low energy mode is a sharp collective excitation of spinons [8], in the high magnetization regime the situation is reversed: the low energy modes in the response form a continuum of psinon excitations (a nomenclature introduced in Ref. [35]) while the high energy mode is a sharp two-magnon bound state.

Discussion.—Our study is complementary to a prior body of work on spectral functions of one dimensional systems beyond conventional Luttinger liquid theory [36,37], which discussed Heisenberg and related chains but focused on zero magnetic field. Other studies in small nonzero magnetic fields were motivated in part by electron spin resonance. The pioneering work of Oshikawa and Affleck noted the irrelevance of backscattering at zero field, and argued that the Larmor theorem shows that it has a negligible effect in small fields [22]. A later study by Karimi and Affleck [38] included nonlinear terms in the fermion dispersion, as well as the effect of the longitudinal part of the backscattering interaction, but not the transverse interactions; hence this misses the formation of the bound state at $k \to 0$.

We are optimistic that these results might be observed in experiment. Indeed there are a number of recent studies that observed spectral features interpreted as Bethe string states via high-resolution terahertz spectroscopy [39] and inelastic neutron scattering [40]. Earlier neutron scattering studies in nonzero magnetic field [41,42] also contain hints of the interaction signatures discussed here. In an ultracold atomic realization of a Heisenberg chain, bound states have been observed by quite different real time protocols [43,44]. The implications of our results for the spectral features at partial polarization to such real time experiments is an interesting direction for future studies.

We would like to thank R. Coldea and L. Motrunich for inspiring remarks and questions, J. S. Caux for pointing out Ref. [6], and M. Kohno for discussions of Ref. [3]. This research is funded in part by the Gordon and Betty Moore Foundation through Grant No. GBMF8690 to UCSB to support the work of A. K. Use was made of the computational facilities administered by the Center for Scientific Computing at the CNSI and MRL (an NSF MRSEC; DMR-1720256) and purchased through NSF CNS-1725797. This work was supported by the NSF CMMT program under Grant No. DMR-1818533 (L. B.) and DMR-1928919 (O. A. S.). We benefitted from the facilities of the KITP, NSF Grant No. PHY-1748958.

pdfelement
The Trial Version

[1] H. Bethe, Z. Phys. **71**, 205 (1931).
[2] G. Müller, H. Thomas, H. Beck, and J. C. Bonner, Phys. Rev. B **24**, 1429 (1981).
[3] M. Kohno, Phys. Rev. Lett. **102**, 037203 (2009).
[4] W. Yang, J. Wu, S. Xu, Z. Wang, and C. Wu, Phys. Rev. B **100**, 184406 (2019).
[5] S. Nishimoto and M. Arikawa, Int. J. Mod. Phys. B **21**, 2262 (2007).
[6] P. Bouillot, C. Kollath, A. M. Läuchli, M. Zvonarev, B. Thielemann, C. Rüegg, E. Orignac, R. Citro, M. Klanjšek, C. Berthier *et al.*, Phys. Rev. B **83**, 054407 (2011).
[7] K. Lefmann and C. Rischel, Phys. Rev. B **54**, 6340 (1996).
[8] L. Balents and O. A. Starykh, Phys. Rev. B **101**, 020401(R) (2020).
[9] U. Schollwöck, Ann. Phys. (Amsterdam) **326**, 96 (2011).
[10] K. Okamoto and K. Nomura, Phys. Lett. A **169**, 433 (1992).
[11] S. Eggert, Phys. Rev. B **54**, R9612 (1996).
[12] ITensor Library, http://itensor.org/.
[13] S. R. White, Phys. Rev. Lett. **69**, 2863 (1992).
[14] G. Vidal, Phys. Rev. Lett. **93**, 040502 (2004).
[15] S. R. White and I. Affleck, Phys. Rev. B **77**, 134437 (2008).
[16] See Supplemental Material at http://link.aps.org/supplemental/10.1103/PhysRevLett.125.187201 for additional numerical results, derivation of the dynamical susceptibility in the low-magnetization regime, and analysis of the two-magnon bound states and spin dynamics in the high-magnetization regime, which includes Ref. [17].
[17] I. Dzyaloshinskii and A. Larkin, Sov. Phys. JETP **38**, 202 (1974).
[18] A. Gogolin, A. Nersesyan, and A. Tsvelik, *Bosonization and Strongly Correlated Systems* (Cambridge University Press, Cambridge, England, 2004).
[19] O. A. Starykh, A. Furusaki, and L. Balents, Phys. Rev. B **72**, 094416 (2005).
[20] V. A. Zyuzin and D. L. Maslov, Phys. Rev. B **91**, 081102(R) (2015).
[21] I. Affleck and M. Oshikawa, Phys. Rev. B **60**, 1038 (1999).
[22] M. Oshikawa and I. Affleck, Phys. Rev. B **65**, 134410 (2002).
[23] A. Klümper and D. C. Johnston, Phys. Rev. Lett. **84**, 4701 (2000).
[24] S. Eggert, I. Affleck, and M. Takahashi, Phys. Rev. Lett. **73**, 332 (1994).
[25] S. Lukyanov, Nucl. Phys. **B522**, 533 (1998).
[26] O. A. Starykh, R. R. P. Singh, and A. W. Sandvik, Phys. Rev. Lett. **78**, 539 (1997).
[27] M. Takigawa, O. A. Starykh, A. W. Sandvik, and R. R. P. Singh, Phys. Rev. B **56**, 13681 (1997).
[28] T. Giamarchi, *Quantum Physics in One Dimension*, International Series of Monographs on Physics (Clarendon Press, Oxford, 2003).
[29] Note that in the noninteracting limit the many-body eigenstates are easily obtained as Slater-determinant states, however, correlations remain nontrivial due to the presence of the string operator [30] and can be calculated using the methods discussed in [31].
[30] E. Lieb, T. Schultz, and D. Mattis, Ann. Phys. (N.Y.) **16**, 407 (1961).

[31] S. Bravyi and D. Gosset, Commun. Math. Phys. **356**, 451 (2017).
[32] M. Nayak, D. Blosser, A. Zheludev, and F. Mila, Phys. Rev. Lett. **124**, 087203 (2020).
[33] A. V. Chubukov, Phys. Rev. B **44**, 4693 (1991).
[34] L. Kecke, T. Momoi, and A. Furusaki, Phys. Rev. B **76**, 060407(R) (2007).
[35] M. Karbach, D. Biegel, and G. Müller, Phys. Rev. B **66**, 054405 (2002).
[36] A. Imambekov, T. L. Schmidt, and L. I. Glazman, Rev. Mod. Phys. **84**, 1253 (2012).
[37] R. G. Pereira, S. R. White, and I. Affleck, Phys. Rev. Lett. **100**, 027206 (2008).
[38] H. Karimi and I. Affleck, Phys. Rev. B **84**, 174420 (2011).
[39] Z. Wang, J. Wu, W. Yang, A. K. Bera, D. Kamenskyi, A. N. Islam, S. Xu, J. M. Law, B. Lake, C. Wu *et al.*, Nature (London) **554**, 219 (2018).
[40] A. K. Bera, J. Wu, W. Yang, R. Bewley, M. Boehm, J. Xu, M. Bartkowiak, O. Prokhnenko, B. Klemke, A. N. Islam *et al.*, Nat. Phys. **16**, 625 (2020).
[41] I. U. Heilmann, G. Shirane, Y. Endoh, R. J. Birgeneau, and S. L. Holt, Phys. Rev. B **18**, 3530 (1978).
[42] M. B. Stone, D. H. Reich, C. Broholm, K. Lefmann, C. Rischel, C. P. Landee, and M. M. Turnbull, Phys. Rev. Lett. **91**, 037205 (2003).
[43] M. Ganahl, E. Rabel, F. H. L. Essler, and H. G. Evertz, Phys. Rev. Lett. **108**, 077206 (2012).
[44] T. Fukuhara, P. Schauß, M. Endres, S. Hild, M. Cheneau, I. Bloch, and C. Gross, Nature (London) **502**, 76 (2013).

pdfelement
The Trial Version